

## ANALYTICAL CALCULATION METHOD FOR REINFORCED CONCRETE COLUMNS UNDER LATERAL IMPACT

*Anatoliy V. Alekseytsev, Valentina M. Tusnina*

National Research Moscow State University of Civil Engineering, Moscow, RUSSIA

**Abstract:** This paper presents an analytical method for the calculation of compressed-bent reinforced concrete (RC) columns subjected to emergency transverse impact, characteristic of relevant anthropogenic hazards such as collisions with vehicles or other impacting objects. The proposed approach accounts for two primary failure mechanisms: flexural failure and diagonal shear failure, and enables the assessment of the ultimate horizontal load capacity, considering the dynamic strengthening of both concrete and reinforcement. The method is based on constructing ultimate capacity curves, which reflect the relationship between the maximum lateral force and the applied axial compressive force. It also introduces coefficients for the confinement of transverse deformations and parameters for the load intensity resisted by the transverse reinforcement. Particular attention is given to modeling the confinement effect on concrete, the influence of the pitch, diameter, and grade of the transverse reinforcement, and the potential for preventing progressive collapse. The proposed methodology serves as an effective tool for analyzing the robustness of buildings and structures under emergency mechanical impacts of anthropogenic origin. The developed approach can be applied in designing preventive measures to enhance column resistance against transverse impacts and contributes to the evaluation of the mechanical safety level of RC structures. This is especially important for columns with high slenderness and for elements with various types of initial or acquired damage.

**Keywords:** reinforced concrete columns, transverse impact, dynamic loading, shear failure, flexural failure, dynamic strengthening, confinement effect, structural safety, progressive collapse, robustness

## АНАЛИТИЧЕСКИЙ МЕТОД РАСЧЕТА ЖЕЛЕЗОБЕТОННЫХ КОЛОНН НА ПОПЕРЕЧНЫЙ УДАР

*А.В. Алексейцев, В.М. Туснина*

Национальный исследовательский Московский государственный строительный университет, г. Москва, РОССИЯ

**Аннотация:** В статье представлен метод аналитического расчета сжато-изогнутых железобетонных колонн, подвергающихся аварийному поперечному удару, характерному для актуальных техногенных воздействий, таких как столкновение с транспортными средствами или другими ударяющими объектами. Предложенный подход учитывает два основных механизма разрушения: по нормальному и по наклонному сечению, и позволяет оценивать предельные значения горизонтальных сил с учетом динамического упрочнения бетона и арматуры. Метод опирается на построение кривых предельной несущей способности, отражающих зависимость максимальных усилий от действующей продольной сжимающей силы, а также вводит коэффициенты стеснения поперечных деформаций и параметры интенсивности нагрузки, воспринимаемой поперечной арматурой. Особое внимание уделено учету стеснения поперечных деформаций бетона, влияния на прочность шага, диаметра и класса поперечной арматуры, а также возможности предотвращения прогрессирующего разрушения конструкции. Предложенная методика служит эффективным инструментом для анализа живучести зданий и сооружений при аварийных механических воздействиях техногенного происхождения. Разработанный подход может быть применен при проектировании профилактических мер, повышающих устойчивость колонн к поперечным ударам, и способствует оценке степени механической безопасности железобетонных конструкций, что особенно важно для колонн большой гибкости и элементов с различными видами начальных или приобретенных повреждений.

**Ключевые слова:** железобетонные колонны, поперечный удар, динамическая нагрузка, разрушение при сдвиге, разрушение при изгибе, динамическое усиление, эффект ограничения, безопасность конструкции, прогрессирующее обрушение, прочность

## 1. INTRODUCTION

**1. Theoretical research review.** The problem of ensuring the bearing capacity of reinforced concrete columns under transverse impact loads is one of the key issues in the field of building and structure safety. Modern theoretical research is focused on developing models that enable the quantitative assessment of the dynamic strength and energy absorption capacity of structures under impulsive loads. The main trends in the theoretical analysis of strength are outlined in many studies. Let us consider some of them.

Article [1] presents a comprehensive analytical model for the dynamic response of axially loaded reinforced concrete columns subjected to transverse impact. The model accounts for the nonlinear interaction of inertial, elastic, and plastic components of the response, as well as the influence of the axial force on damage progression. The authors demonstrated that an increase in axial force accelerates damage accumulation and reduces the residual load-bearing capacity, which has direct implications for safety analysis under impact. In [2], an analytical approach was proposed to assess the response of both reinforced concrete and composite columns under lateral impact. The method is based on a simplified elastoplastic response theory and allows for differences in the energy absorption capacity of reinforced and composite elements. The work emphasizes that combining reinforcement with composite materials enhances not only impact resistance but also the column's ability to maintain its shape until failure, which is critical for preventing progressive collapse. The authors of [3] investigated resistance mechanisms and developed a methodology for analyzing the reliability of reinforced concrete columns under lateral impact. Their results showed that structural safety under such impacts depends on the interaction of flexural and shear failure mechanisms, as well as the nature of impact energy transmission through the reinforcement. The authors proposed introducing a dynamic

stability coefficient to estimate the probability of exceeding ultimate deformations. Research [4] contributes to the field by assessing the residual strength of corrosion-damaged elements. Their models showed that the degradation of reinforcement and concrete properties significantly reduces the impact toughness and damping capacity of columns, which is particularly important when considering progressive collapse scenarios. Article [5] proposes a simplified method for predicting the degree of damage in circular reinforced concrete columns under axial load and lateral impact. The model is based on the principles of equivalent stiffness and plastic deformation energy, allowing for the estimation of the threshold between elastic and catastrophic response. A number of works address the influence of axial load on the nonlinear response of elements. For instance, [6] showed that an increase in compressive force intensifies local instability and leads to brittle failure modes. Similar results are presented in [7], which highlights the dependence of the failure mechanism on the impact type: bending deformations dominate under soft impact, whereas shear damage prevails under hard impact. Theoretical studies [8] extend strength analysis to elements damaged by corrosion and subjected to impulsive transverse loads. Similar works note that accounting for cross-section degradation and reduced bond between reinforcement and concrete leads to a significant reduction in the load-bearing capacity reserve, especially under short-term, high-intensity pulses. Work [9] demonstrates that bending deformations and stability loss depend not only on geometric parameters and reinforcement but also on boundary conditions, enabling the refinement of computational models for real-world operating conditions.

Thus, modern theoretical research is focused on refining physic-mechanical models of failure, introducing dynamic safety factors, and developing approximate methods for assessing the load-bearing capacity of reinforced concrete elements under short-term transverse impacts.

**2. Experimental research.** Experimental data play a key role in verifying theoretical models and ensuring the reliability of calculations for the design of impact-resistant structures. Systematic testing of columns under transverse impact is presented in works such as [10], which investigated the behavior of square columns under axial compression and low-velocity lateral impact. The authors identified characteristic response stages—from elastic bending to crack formation and diagonal shear failure. In [11], the authors conducted a series of experiments to determine the residual load-bearing capacity of circular columns after impact. The results confirmed that up to 70% of the initial bearing capacity can be preserved under moderate impact energies, which is highly significant for assessing building safety after partial damage. Article [12] investigated the influence of reinforcement percentage on column resistance to lateral impact. The experiments showed that increasing the reinforcement ratio enhances the ultimate energy absorption, but this effect saturates beyond a certain level. The authors of [13] compared the results of physical tests and numerical modeling, revealing a high correlation in deformation distribution and response velocities. Their subsequent work [14] enabled a detailed examination of the damage formation process under repeated impacts, which is particularly important for analyzing progressive collapse in emergency scenarios. Article [15] focused on columns with insufficient shear reinforcement. Their experiments revealed a sharp reduction in energy absorption capacity and strength when shear failure mechanisms prevailed. In [16], a study was conducted on the nonlinear response and shear behavior of columns under lateral impact. The experiments showed that the transition from a flexural to a shear mechanism is accompanied by localized concrete crushing and loss of section stability. Composite reinforcement is also actively investigated. The authors of [17] studied the use of GFRP bars in reinforced concrete columns under lateral

impact. The experiments demonstrated improved energy absorption and failure resistance compared to traditional steel reinforcement. Researchers [18] showed that external strengthening with carbon fiber-reinforced polymer (CFRP) significantly enhances the ability of columns to resist static and impact lateral loads, preventing loss of bearing capacity and providing a structural damping effect. Experimental data on the dynamic response of reinforced concrete elements, obtained in [19], demonstrate similar patterns of impact energy redistribution and the role of reinforcement stiffness in preventing through-failure. Thus, experimental research confirms the significant influence of geometry, reinforcement, prestressing, defects, damage, and external strengthening on the ability of columns to withstand transverse impact loads.

**3. Dynamics, Damping, and Protection Against Progressive Collapse.** Dynamic aspects of reinforced concrete column behavior under impact loads are related to the processes of energy transfer and dissipation, which largely determine the likelihood of progressive collapse. The most important aspect here is the accounting for damping. The authors of [20] proposed a modified Rayleigh damping function for the numerical simulation of internal damping in frame structures. Subsequently, colleagues in [21] advanced this approach by proposing a non-stationary time-domain model of dynamic deformation that accounts for the material's delayed response. This allows for more accurate reproduction of oscillatory processes and critical states of reinforced concrete elements. The work of the authors [7] examines the dynamic behavior of columns under soft impacts and proposes criteria for damage assessment based on strain rate and residual stiffness. The authors emphasize that the structure's ability to dissipate energy through microcracking plays a key role in preventing progressive collapse. Research [15] showed that a lack of shear reinforcement sharply reduces the ability of columns to dampen impact energy, leading to rapid, cascading failure and loss of

load-bearing capacity in adjacent elements. These results are complemented by data from [16], which noted that proper design of transverse reinforcement can ensure a controlled plastic deformation mechanism, preventing instantaneous (brittle) failure.

Thus, modern approaches to ensuring dynamic stability rely on a combination of constructive measures, numerical modeling of damping, and analysis of nonlinear response, all aimed at preventing sequential (chain) failures. The conducted literature analysis demonstrates that research on the behavior of reinforced concrete columns under transverse impact is rapidly evolving towards the integration of theoretical, experimental, and computational approaches. Despite significant achievements, tasks related to the simple and rapid safety assessment of reinforced concrete elements, particularly columns, based on engineering methods remain unsolved. One such method is proposed in this article.

## 2. METHODS

*2.1 Problem formulation.* Let us consider a column made of heavy-weight concrete with steel reinforcement, subjected to a compressive axial force, where the influence of the bending moment is negligible. That is, the column can be conventionally considered as eccentrically compressed with a small eccentricity. As a result of an anthropogenic event, the column is subjected to an emergency impact. This impact could be initiated by a collision with a vehicle or another impacting body. For this scenario, the limit state condition of the first group will be as follows:

$$f(N(t), F_h(t)) \leq f(N(t), Q(t), M(t))_{ult} \quad (1)$$

where:  $f()$  is load effect functional;  $N(t), F_h(t)$  are longitudinal forces and transverse loads varying in time;  $f()_{ult}$  is resistance functional of the column in the limit state;  $N(t), Q(t), M(t)$  are ultimate longitudinal force, ultimate resultant transverse force, ultimate resultant

(principal) moment that the reinforced concrete structure can withstand.

The dynamic loading process for analytical calculation can be represented by equations incorporating maximum static forces adjusted for dynamic effects and possible dynamic overloading:

$$\begin{cases} k_{d1} N_{\max} \leq N_{cd,ult} \\ k_{d2} M_{\max} \leq M_{cd,ult} \\ k_{d3} Q_{\max} \leq Q_{cd,ult} \end{cases}, \quad (2)$$

where  $k_{d1}, k_{d2}, k_{d3}$  – coefficients accounting for dynamic effects under emergency impact;  $N_{\max}$ ,

$Q_{\max} = \sqrt{Q_x^2 + Q_y^2}$ ,  $M_{\max} = \sqrt{M_x^2 + M_y^2 + M_z^2}$  are longitudinal force, principal transverse force, and principal moment induced by the combined (service and emergency) loads;  $N_{cd,ult}$ ,  $Q_{cd,ult}$ ,

$M_{cd,ult}$  are corresponding internal forces resisted by the structural materials, considering dynamic strengthening.

Under the assumption that the force impact on the column does not cause extensive local damage leading to global failure (i.e., effects such as punching or scabbing are absent, which may occur at relatively low impact velocities during the contact between the impactor and the column), failure is expected to occur either in the normal section (Fig. 1a) or in the inclined section (Fig. 1b).

It is assumed that the ultimate values of the horizontal load nonlinearly depend on the magnitude of the compressive axial force for both flexural failure and shear failure mechanisms. This relationship is described by the ultimate load capacity curve (Fig. 1c), which demonstrates that under the same service compressive force  $N_e$ , the maximum loads preceding flexural failure  $F_{1,ult}$  and shear failure  $F_{2,ult}$  differ. If a given load combination  $F_h$  lies below these curves, the column maintains its load-bearing capacity under the actual force  $N_e$ .

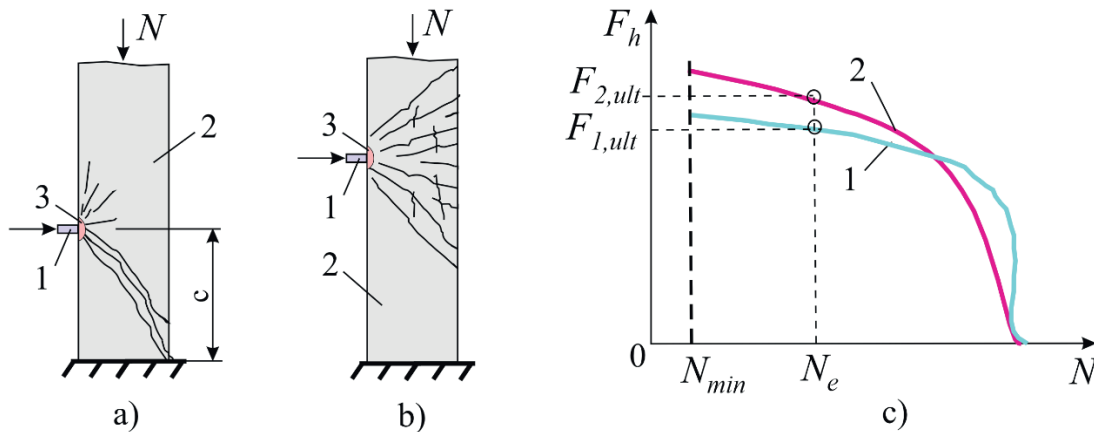


Figure 1. Problem formulation: failure schemes under horizontal impact - diagonal shear failure (a); flexural failure (b); 1 - impactor, 2 - reinforced concrete column, 3 - concrete crushing zone; ultimate capacity curves (c); 1 - moment failure, 2 - shear failure

## 2.2 Calculation Methodology for Normal Sections

For the analytical substantiation of the column's strength with respect to the inclined section, the general strength condition and the specific inequality derived from it are used:

$$F_h(N_e, t) \in \Omega \leq F_h(N_e)_{ult} \in L_{BC} \rightarrow \rightarrow (F_{h,max} \leq F_{h,ult}) \Big|_{N=N_e}, \quad (3)$$

where  $F_h(N_e, t)$  – horizontal force from emergency impact at the actual value of  $N_e$  at time  $t$ ;  $\Omega$  – range of permissible emergency load values;  $F_h(N_e)_{ult}$  – ultimate horizontal force resisted by the reinforced concrete column in the critical normal section, considering dynamic strengthening of materials under the condition  $N = N_e$ ;  $L_{BC}$  – curve of the ultimate values of this force.

Thus, to assess the section strength, it is necessary to construct the ultimate load capacity curve. Let us define this curve by characteristic points  $A, B_i, C$ . We assume that point  $A$  is located at the conditional intersection of curve 1 with the  $Q$ -axis (Fig. 1c). Suppose the longitudinal force in the column cannot be zero, and its value is  $N_{min}$  (e.g., the self-weight of the column). At this point, the horizontal impact is

maximal. Point  $C$  is located at the intersection with the  $N$ -axis. Here, the horizontal impact is minimal under the maximum compressive longitudinal force. Points  $B_i, i=1..n$  are intermediate and describe the shape of the curve. Let us consider the construction of this curve.

Point A,  $F_h = 0, :$

$$k_{d1}N_A(\lambda) = \begin{cases} \pi^2 E_b I_{red} / l_0^2, \lambda > 50; \\ \varphi [R_b A_b + R_{sc} A_{s,tot}], \lambda \leq 50 \end{cases}, \quad (4)$$

Here:  $l_0 = \mu l$  – design length, accounting for the variation in the geometric length  $l$  of the column depending on its support conditions (considered through the coefficient  $\mu$ );  $R_{sc}, A_{s,tot}, R_b, A_b$  – design strengths and cross-sectional areas of reinforcement and concrete, respectively;  $\varphi$  – coefficient determined according to SP 63.13330 for the case of small eccentricities of the compressive force;  $\lambda$  – slenderness of the column.

Condition (4) specifies that slender columns lose their load-bearing capacity due to Euler buckling instability, while conventionally designed columns are primarily governed by material strength. Calculations have shown that for columns with  $\lambda \leq 50$  and under transverse impact,  $k_{d1} \rightarrow 1$ .

Points  $B_1 - B_n$ . After calculating the ultimate value  $N_A = N_{ult}$  using (4), values  $N_{e,i}$  are assigned, for which the ultimate values  $P_{i,ult} \in L_{BC}$  are computed. For each value  $N_{e,i}$ , the depth of the concrete compression zone  $x$  in the critical section is calculated, and equilibrium equations are formulated considering a unit horizontal load. Subsequently, its ultimate value is determined. This can be expressed as:

$$x = x_m + \frac{I_{red} N_{e,i}}{A_{red} M},$$

$$x_m = \sqrt{\alpha_s^2 (\mu_s + \mu'_s)^2 + 2\alpha_s (\mu_s + \mu'_s a' / h_0)} - \alpha_s (\mu_s + \mu'_s). \quad (5)$$

$$\alpha_s = \frac{0.0015 E_s}{R_{b,ser}}, \mu_s = \frac{A_s}{bh_0}, \mu'_s = \frac{A'_s}{bh_0},$$

$$M = M_f + M_e. A_{red} = bh + \frac{E_s}{E_b} (A_s + A'_s);$$

Here:  $M_f$  – bending moment from service loads;  $M_e$  – moment caused by the longitudinal force due to accidental eccentricity. Other designations of calculated parameters are generally accepted and provided in SP 63.13330. The equilibrium equation under a unit horizontal load for a rectangular column section is as follows:

$$M_{\max,i} + N_{e,i} e_f = k_1 R_b \cdot b \cdot h_0^2 \cdot \alpha_R + k_2 R_{sc} \cdot A'_s \cdot (h_0 - a)$$

$$M_{\max} = \max \left\{ \left( M_f + M(\bar{F}_h) + M_e \right) \right\} \quad (6)$$

$$e_f = \frac{1}{1 - N_{e,i} / N_A |_{\lambda > 50}} \left( f + \frac{h_0 - a'}{2} \right).$$

Where  $k_1, k_2$  are the dynamic strengthening coefficients of concrete and reinforcement, respectively;  $M(\bar{F}_h)$  is the moment from the

horizontal load  $\bar{F}_h = 1$ ,  $e_f$  is the eccentricity of the force  $N_{e,i}$  considering the deflection  $f$ , induced by the force  $\bar{F}_h$ .

The deflection  $f$  is determined considering the curvature  $1/r$  of the element and its stiffness. The stiffness for a rectangular cross-section element is calculated using the known formula:

$$D = \frac{0.15 E_b I_b}{\varphi_l (0.3 + \delta_e)} + 0.7 E_s I_s \quad (7)$$

where:  $E_b, I_b$  – initial modulus of elasticity and moment of inertia of concrete;  $\varphi_l$  – coefficient accounting for the duration of load action, taken as 1 for this design case;  $\delta_e$  – relative eccentricity, taken as 0.15 for the case of small eccentricities;  $E_s, I_s$  – modulus of elasticity and moment of inertia of reinforcement.

The deflection of the column when divided into  $m$  sections of equal length  $\Delta l$  is then

$$f = \sum_{j=1}^m \int_0^{\Delta l} M(\bar{F}_h)_j \left( \frac{1}{r} \right)_j dz =$$

$$= \frac{1}{D} \sum_{j=1}^m \int_0^{\Delta l} M(\bar{F}_h)_j \times M(\bar{F}_h)_j dz \quad (8)$$

where  $D$  is the element stiffness, and the product of the sub integral functions can be evaluated using Simpson's formula. Solving equations (6) yields the value  $k_{d2} P_{i,ult}$ .

Point C. The value  $P_{ult}$  is determined from the condition:

$$k_{d2} M_{\max}(P_{ult}) \leq M_{ult} \quad (9)$$

where  $M_{\max}(P_{ult})$  is the maximum bending moment in the section from the vertical force,  $M_{ult}$  is the ultimate moment resisted by the reinforced concrete section under bending. For a rectangular section, it is determined conventionally:

$$M_{ult} = k_1 R_b \cdot b \cdot h_0^2 \cdot \alpha_R + k_2 R_{sc} \cdot A'_s \cdot (h_0 - a). \quad (10)$$

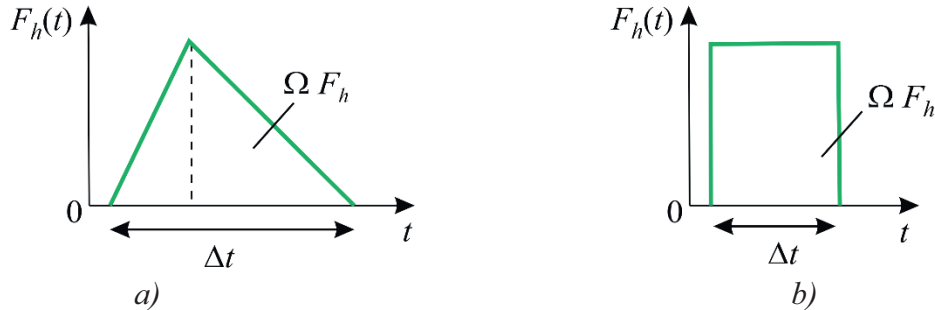


Figure 2. Pulse shapes under dynamic loading: triangular (a), rectangular (b)

the loads without considering their duration. To compare the values of loads specified as impulses with those obtained from the mentioned equations, the following formula can be used:

$$P = \Omega F_t / \Delta t, \quad (11)$$

where  $\Omega F_t$  is the area under the pulse,  $\Delta t$  is the actual impact duration on the structure.

### 2.3 Calculation Method for Inclined Sections.

Under dynamic impact on a column, particularly in the presence of rigid restraints at the supports, the strength of the inclined section may be exhausted either by the action of the transverse force or by the bending moment. The curve  $L_{BC}$  is constructed without specific characteristics for different values of  $N_{e,i}$ , following the methodology below. To assess the strength of the inclined section, the system of inequalities is written as:

$$\begin{cases} \left( \frac{\Delta Q_d}{k_N^d Q_d^{ult}} \pm \frac{Q_{st}}{Q_{bN} + Q_{swN}} \right) \leq 1, \\ M_{\max} \leq M_b + M_{sw} + M_{s,inc} \end{cases}, \quad (12)$$

where the first equation is necessary to determine the value of  $F_h$  based on the dynamic increment of transverse force  $\Delta Q_d$ , while the

Dynamic loads can have various pulse shapes (Fig. 2), while equations (6) and (9) allow determining the dynamic equivalents of

second serves a verification function. Here, in the first equation,  $k_N^d$  is a coefficient accounting for the level of compressive force, confinement of transverse deformations, and the kinematic constraints of the column. The quantities  $Q_d^{ult}, Q_{st}, Q_{bN}, Q_{swN}$  are represent the transverse forces resisted by the section under dynamic loading, static service loading, concrete under service loads, and reinforcement under service loads, respectively. In the second equation,  $M_b, M_{sw}, M_{s,inc}$  denote the bending moments resisted by concrete, longitudinal reinforcement, transverse reinforcement, and inclined bars (bent-up bars), respectively.

The ratio  $k_N^d$ :

$$k_N^d = \begin{cases} \frac{1}{\sqrt{1,5 - \mu}} \left( k_e + \left( \frac{N_e}{N_{ult}} \sqrt{\frac{P_{Ne}^{ult}}{P_{ult}}} \right) \right)^{-1}, \\ \text{for } \frac{N_e}{N_{ult}} < 0.6, \\ \left( \frac{P_{Ne}^{ult}}{P_{ult}} + k_e \right)^{-1}, \text{ for } \frac{N_e}{N_{ult}} \geq 0.6, \end{cases}, \quad (13)$$

where  $P_{Ne}^{ult}$  is the value of transverse impact load initiating flexural failure under force  $N_e \neq 0$ ,  $P_{ult}$  is the same under force  $N_e = 0$ .

The value of  $N_{ult}$  is determined using the second equation of system (4);  $k_e$  is the coefficient of transverse deformation confinement.

For a square section, it can be determined using Fig. 3 and the dependency provided below.

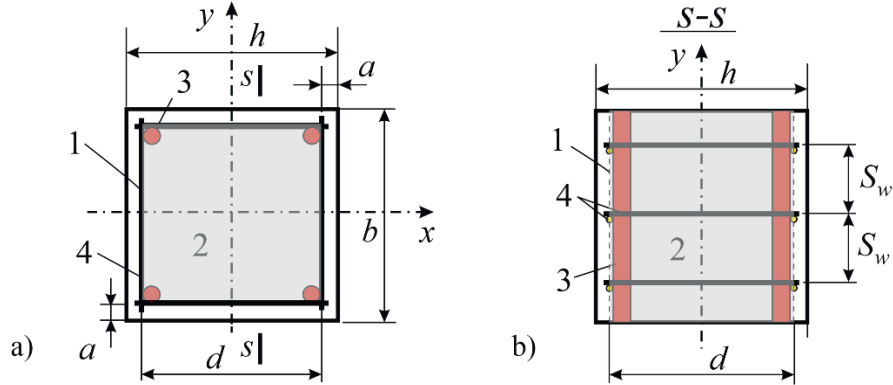


*Figure 3. Determination of the deformation confinement level: column cross-section (a); section s-s (b); 1 – boundary of the deformation confinement zone, 2 – core of the deformation confinement zone, 3 – longitudinal reinforcement, 4 – transverse reinforcement*

where  $\mu_{sc}, d_w$  are the reinforcement percentage considering core area 2 and the area of longitudinal reinforcement only, and the diameter of the transverse reinforcement bar;  $d$  is the length of the transverse bar in the impact plane, as shown in Fig. 3.

When the projection length of the inclined section onto the vertical axis does not exceed twice the effective depth of the section, the following formula is proposed for  $Q_d^{ult}$ :

$$Q_d^{ult} = \sqrt{3k_1 R_{bt} (1 + k_e)^{(1 + \sqrt{N_e / N_{ult}})} b h_0^2 q_{sw}^d}, \quad (15)$$

where  $R_{bt}$  – design tensile strength of concrete,  $b, h_0$  – width and effective height of the section,  $q_{sw}^d$  – distributed per length load resisted by transverse reinforcement under impact, within the vertical projection of the inclined section. It is defined as:

$$k_e = \frac{1}{1 - \mu_{sc}} \left( 1 - \frac{S_w - d_w}{2d} \right)^2, \quad (14)$$

$$q_{sw}^d = k_2 \frac{R_{sw} A_{sw}}{S_w} \left( 1 - (0.2 + k_e) \frac{N_e}{N_{ult}} \right), \quad (16)$$

The value of  $Q_{bN}$  in formula (12):

$$Q_{bN} = 1.5 \varphi_n R_{bt} b h_0^2 / c, \quad (17)$$

$$0.5 \varphi_n R_{bt} b h_0 \leq Q_{bN} \leq 2.5 R_{bt} b h_0$$

where  $c$  – projection of the inclined section onto the vertical axis,  $c$  is calculated as:

$$c = \sqrt{\frac{1.5 \varphi_n R_{bt} b h_0^2}{0.75 q_{sw}^c}}, \quad c \leq 2h_0,$$

$$\varphi_n = \begin{cases} 1.25, & 0.25R_b \leq \sigma_b < 0.5R_b \\ 2.5 - \left( 1 - \frac{\sigma_b}{R_b} \right), & 0.5R_b \leq \sigma_b \leq R_b \end{cases}, \quad (18)$$

$$\sigma_b = \frac{N_e}{A_b + \frac{\alpha E_b \varepsilon_{b0}}{R_b} A_{sc}}.$$

All notations in the formula are standard and provided in SP 63.13330, the value of  $q_{sw}^c$  is determined by (16), assuming that  $k_2 = 1$ .

### 3. RESULTS

**3.1. Comparison with Experiment. Calculation for Normal Section.** To verify the proposed method, we use the experimental results from [10], shown in Fig. 4. For the calculation, in accordance with recommendations from various studies, including [8], we adopt the following

dynamic strengthening coefficients for materials:  $k_1=1,15$ ,  $k_2=1,2$ ,  $k_{d2}=1.5$ . The load is considered as suddenly applied with a rectangular pulse shape. The distance between the supports is 1.38 m,  $\alpha = E_s / E_b = 6.66$ . The equilibrium equation (10) applied to this experimental task is

$$M_{\max} + Ne_f = k_1 R_b \cdot b \cdot h_0^2 \cdot \alpha_R + k_2 R_{sc} \cdot A'_s \cdot (h_0 - a')$$

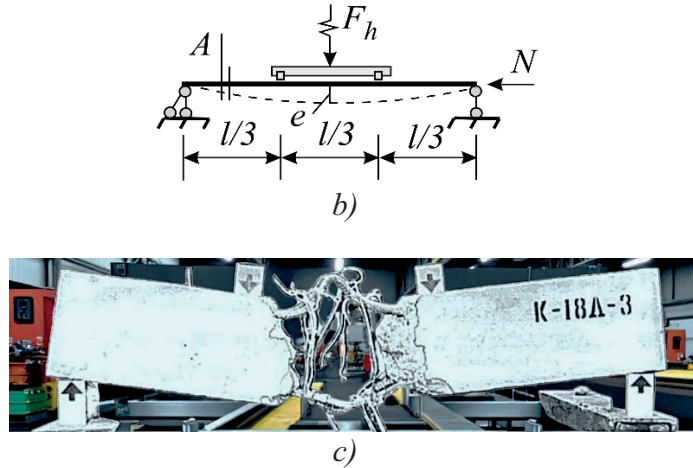
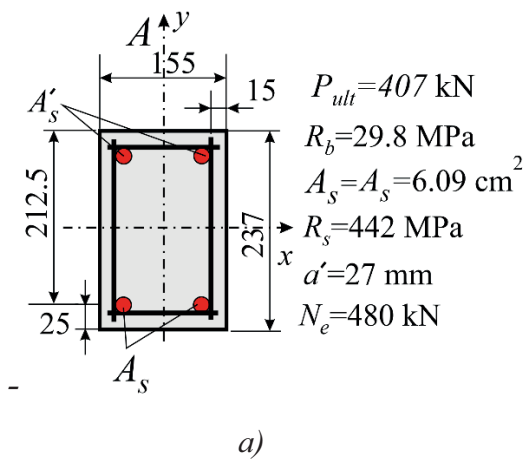


Figure 4. Experimental data for verification of the calculation methodology: material and load characteristics, cross-section in the experiment (a), design model (b), the crushed specimen (c)

The boundary values of the relative height of the concrete compression zone under bending are calculated as

$$\xi_R = 0,8 / (1 + (442 / 2 \cdot 10^5) / 0,0035) = 0,49,$$

$\alpha_R = 0,49(1 - 0,49/2) = 0,37$ . The bending moment is  $M_{\max} = F_h \cdot 1,38 / 6 = 0,23 F_h$  (kHm).

The eccentricity  $e_f$  is calculated using (6). For this, the moment of inertia and Euler force are determined:

$$I_{red} = 23,7^3 \cdot 15,5 / 12 + 6,66 \cdot 2 \cdot 6,09 \cdot (18,5 / 2)^2 = 24134 \text{ cm}^4.$$

$$N_A = \pi^2 \cdot 3 \cdot 10^7 \cdot 24134 \cdot 10^{-8} / 1,38^2 = 37520 \text{ kN}.$$

The system deflection is determined using Mohr integrals:

$$f = 207 F_h l^3 / 11164 E_{red} I_{red} = F_h \cdot 207 \cdot 1,38^3 10^6 / 11164 \cdot (48 \cdot 0,85 \cdot 3000 \times 24134) = F_h \cdot 0,01774 \text{ cm}.$$

$$e_f = 1 / (1 - 480 / 37520) (F_h \cdot 0,01774 + 18,5 / 2) = 9,361 + 0,0181 F_h.$$

Substituting all values into equation (10), we have  $31,68 F_h = 8489 + 5975 - 4493$ ,  $F_h = 314 \text{ kN}$ ,  $P = F_h \cdot 1,5 = 314 \cdot 1,5 = 471 \text{ kN}$ . The theoretical result satisfactorily corresponds to the experimental one. The error is less than 15.7%.

3.2. *Example of Column Calculation for Inclined Section.* Let a column (Fig. 5, a) be subjected to an emergency impact load  $P$ . The structure is made of concrete with compressive strength class B25 ( $R_b = 11,5 MPa$ ,  $R_{bt} = 0,9 MPa$ ), reinforcement A500 ( $R_s = 435 MPa$ ,  $R_{sw} = 300 MPa$ ), with dynamic strengthening coefficients as in Section 3.1:  $k_1 = 1,1$ ,  $k_2 = 1,2$ , and coefficient  $\mu = 0,7$ . The longitudinal reinforcement area is  $4\phi 28$   $A_{sc0}^{4\phi 28} = 24,63 cm^2$ , and the transverse reinforcement consists of  $4\phi 8$  bars forming a

closed contour, spaced at 250 mm along the height  $A_{sw}^{d8} = 0,503 cm^2$ . The load is  $N_e = 2000 kN$ , and the transverse force (under conditionally centered loading of the middle column) is  $Q_{st} = 0 kN$ . It is necessary to evaluate the maximum bearing capacity of the column under horizontal impact. The given load arrangement suggests that the most probable failure mechanism will be the loss of strength of the inclined section (Fig. 5, c). Taking this and the above loading into account, we write (12) in the form  $\Delta Q_d \leq k_N^d Q_d^{ult}$ .

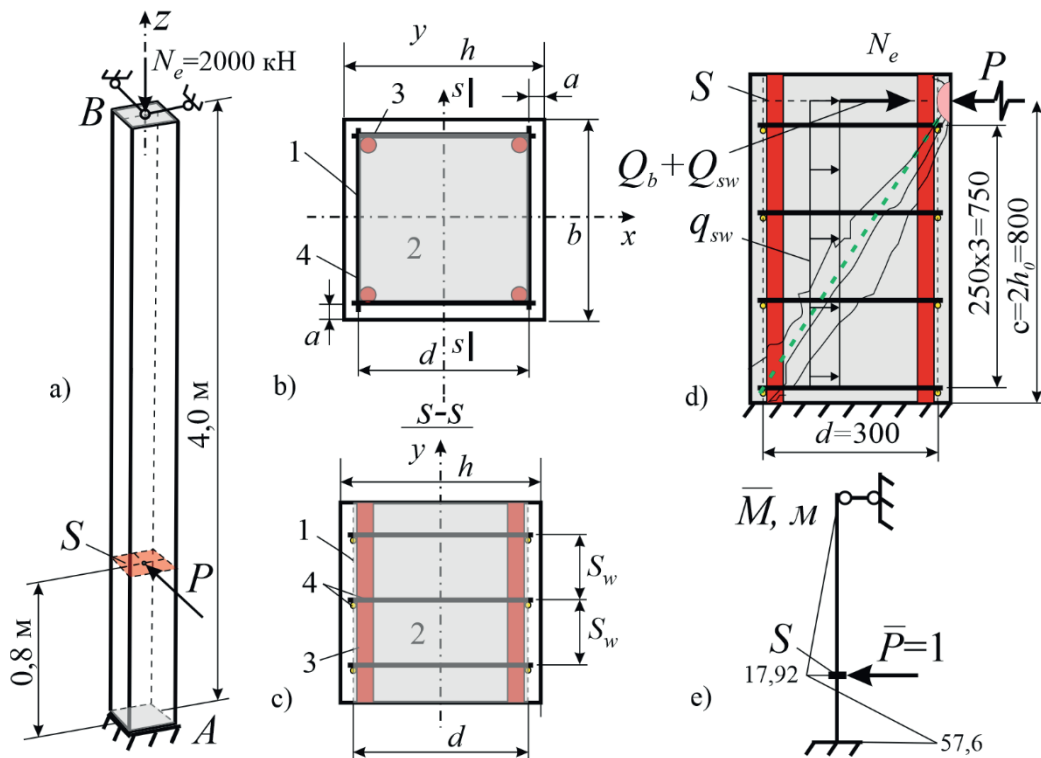


Figure 5. Reinforced concrete column with calculation parameters: design model (a), cross-section  $S$  (b); 1 - contour of the deformation confinement zone, 2 - core of this zone, 3 - longitudinal reinforcement, 4 - transverse reinforcement; cross-section  $s-s$  (c), inclined section (shear) failure scheme (d), bending moment diagram caused by unit impact (e)

It is calculated:  $\mu_{sc} = 24,63 / 30 \cdot 30 = 2,73\%$ ,  $d = 30$  cm - the dimension of the deformation confinement zone (Fig. 5, b, c). It is solved (14):

$$k_e = \frac{1}{1 - \mu_{sc}} \left( 1 - \frac{S_w - d_w}{2d} \right)^2 = \frac{1}{1 - 0,0273} \left( 1 - \frac{25 - 2,8}{2 \cdot 30} \right)^2 = 0,408,$$

$$N_{ult} = \varphi(R_b A_b + R_{sc} A_{sc0}) = 0.9(1.15 \cdot 40 \cdot 40 + 43.5 \cdot 24.64) = 2620 \text{ kN}$$

The ratio  $N_e / N_{ult} = 2000 / 2620 = 0,763 \geq 0,6$ , therefore in formula (13) using the last equality. Next, it is determined the ultimate horizontal forces for flexural failure at forces  $N_e = 0 \text{ kN}$ ,  $N_e = 2000 \text{ kN}$ . For the bottom support fixation, the equation (12) is:

$$M_{\max} + N_e e_f = k_1 R_b \cdot b \cdot h_0^2 \cdot \alpha_R + k_2 R_{sc} \cdot A_{sc}^{2d28} \times (h_0 - a).$$

The maximum moment is determined from Fig. 5, e, with the value  $e_f = ((35 - 5) / 2) = 15 \text{ cm}$ . The value  $\alpha_R$ , ensuring the absence of brittle failure, is determined in the conventional way:

$$\xi_R = 0,8 / (1 + (435 / 2 \cdot 10^5) / 0,0035) = 0,493, \\ \alpha_R = 0,493(1 - 0,493 / 2) = 0,37.$$

Solving equation (12), it is obtained:

$$0,144 \cdot 400 P_{Ne}^{ult} + 2000 \cdot 15 = 1,1 \cdot 1,15 \cdot 40 \cdot 35^2 \times 0,37 + 1,2 \cdot 43,5 \cdot 12,32 \cdot (35 - 5) \rightarrow$$

$\rightarrow P_{Ne}^{ult} = 212,74 \text{ kN}$ . When solving the same equation for  $N_e = 0 \rightarrow P_{ult} = 733,1 \text{ kN}$ , next,  $k_N^d = (0,403 + 212,74 / 733,1)^{-1} = 1,4427$ . Thus, it is determined the value  $q_{sw}^d$ , considering the impact resistance provided by the 2d8 lateral rebars (5):

$$q_{sw}^d = 1,2 \cdot \frac{30 \cdot 1,01}{25} \left( 1 - (0,2 + 0,403) \left( \frac{2000}{2620} \right) \right) = 1,4544(1 - 0,422) = 0,78493 \text{ kN / cm}.$$

The constructive requirement is checked:  $q_{sw}^d \geq q_{sw,\min}$ . For this, it is calculated the elasticity coefficient:

$$\nu_b = R_b / E_{b0} \varepsilon_b = 11,5 / (27,5 \cdot 0,002 \cdot 10^3) = 0,209$$

Normal stresses

$$\sigma = N / A_{red} = 2000 / (40 \cdot 40 + 0,209^{-1} \times (2 / 2,75) \cdot 10 \cdot 24,64) = 1,017 \text{ kPa};$$

$$\varphi_n = 2,5 \left( 1 - \frac{\sigma}{R_g} \right) = 2,5 \left( 1 - \frac{1,017}{1,15} \right) = 0,289;$$

$$q_{sw}^d \geq q_{sw,\min} = 0,25 \varphi_n R_{bt} b = 0,25 \cdot 0,289 \cdot 0,09 \cdot 40 = 0,2601.$$

The condition is satisfied. The ultimate value of the dynamic transverse force using expression is (4):

$$Q_d^{ult} = \sqrt{3 \cdot 1,1 \cdot 0,09 \cdot (1 + 0,403)^{(1 + \sqrt{2/2,62})} \times \times 40 \cdot 35^2 \cdot 0,7849} = 146,8 \text{ kN}.$$

The value

$$\Delta Q_d = Q_d^{ult} \cdot k_N^d = 146,8 \cdot 1,4427 = 211,8 \text{ kN}.$$

This value of the horizontal dynamic force is the ultimate at  $N_e = 2000 \text{ kH}$ .

**3.3 Numerical Verification of Calculation Results.** Let us perform a calculation of a solid finite element model, Fig. 6.

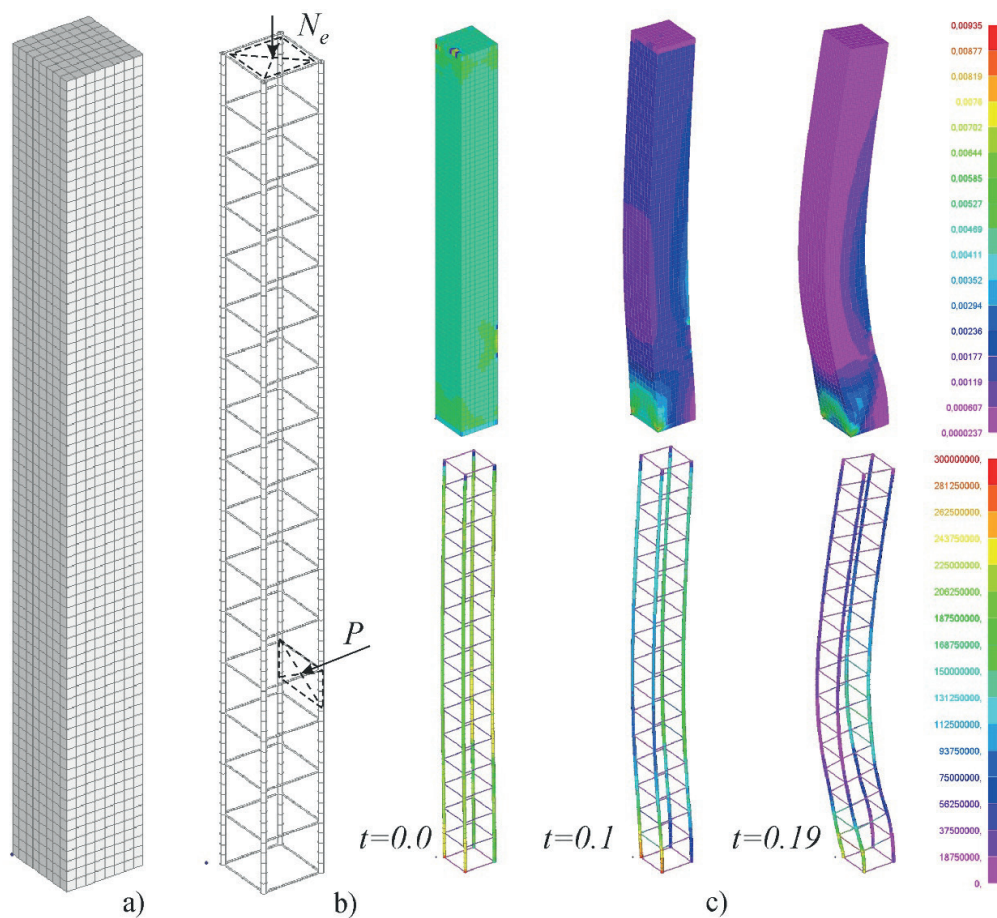


*Figure 6. Some results of the numerical analysis: solid finite elements of concrete (a), bar elements of reinforcement (b), results of the assessment of shear strains in concrete and von Mises equivalent stresses in the reinforcement; the scales are given for time 0.19 s*

Concrete was represented as hexahedral elements deforming according to the Drucker-Prager model with the capability to simulate element failure. Reinforcement was modeled as bars following bilinear diagrams. The characteristics of concrete used in the calculation are as follows: cohesion stress 3.3 MPa, internal friction angle 38 deg., dilation angle 28 deg., tensile stress 0.9 MPa, compressive stress 11.5 MPa, ultimate tensile strain 0.0001, ultimate compressive strain 0.0035. For the reinforcement, the following was adopted: ultimate tensile strain 0.025, yield stress of longitudinal bars 435 MPa, yield stress of transverse bars 300 MPa.

The parameters of the computational process are as follows: overall damping – 5%; when solving the nonlinear problem, 25 iterations of the

Newton-Raphson method were used at each integration step, with stiffness matrix updates every 5 iterations. The convergence criterion was set as a tolerance for nodal force residual equal to 0.1%. The integration time was taken as 1.5 sec, with a step  $\Delta t = 0,05$  sec .

Analysis of Figure 6 allows us to note the following features. When resisting only the longitudinal force at time  $t = 0.0$  sec before the impact, the stresses in the longitudinal reinforcement are significantly lower than when assessed using the formula from SP 63.13330, while concrete, conversely, carries most of the load. During the realization of the impact, which is accompanied by an increase in the value of  $P$  at time  $t = 0.1$  sec, a wave of deformations corresponding to the flexural failure mechanism initially forms, and an increase in equivalent

stresses is observed in both longitudinal and transverse reinforcement. In the limit state at  $t = 0.19$  sec, the shear strains in concrete exceed the limits for elastic behavior, meaning cracks form. In addition to the fan of cracks along the inclined section, cracks caused by bending and shear also form on the impact side along the height of the column. The stresses in the longitudinal reinforcement at this point are at the level of 50% of the design resistance, while the transverse reinforcement undergoes plastic deformation with stresses equal to  $R_{sw} = 300$  MPa. This indicates the initiation of the shear failure mechanism. Significant plastic deformations of these bars lead to a substantial reduction in bearing capacity and the formation of a kinematically unstable system. A comparison of the ultimate compressive force is performed. The analytical method gives  $N_{ult} = \varphi(R_b A_b + R_{sc} A_{sc0}) = 2620$  kN (calculated above). The calculation of the solid FEM model yielded a value of 2778 kN. For the column under consideration, the load-bearing capacity curves using points  $(N_e; P_{i,ult}) \in L_{BC}$  (see Fig. 1, c) is constructed. The results are presented in Fig. 7. The figure shows that the scope of the methodology is  $0.14 \leq N_e / N_{ult} \leq 0.8$ , however, with a column strength reserve of less than 20%

and during an emergency situation, it will most likely fail, so the necessity of calculation in this range is not in demand for practice; usually, columns, based on structural considerations (bearing possibilities), have a strength reserve of 30-50%.

#### 4. DISCUSSION AND DIRECTIONS FOR FURTHER RESEARCH

The proposed methodology describes one of the possible failure scenarios for a column. In this case, the dynamic load increases gradually at a low rate, and the stresses in the concrete do not exceed the value corresponding to its local crushing strength. The strain rate also remains below the critical level; therefore, fan-shaped cracks do not form, and there is no spalling or punching of concrete in the contact zone. Design models for compressed elements, including those presented in regulatory documents, do not yet account for a number of important effects. These include concrete dilation, energy dissipation during the dynamic process and its consideration in modeling, confinement of transverse concrete deformations, and the emergence of additional stresses in the transverse reinforcement due to this confinement.

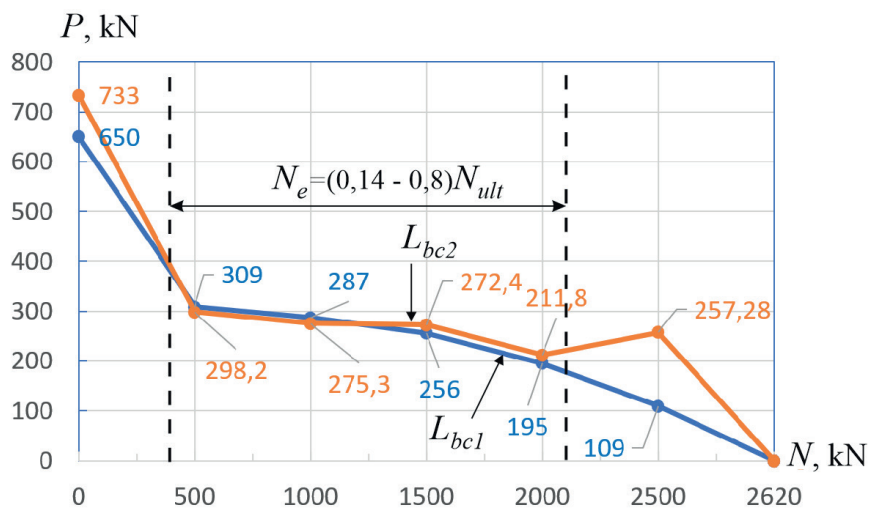


Figure 7. Load-bearing capacity curves of the column:  $L_{bc1}$  – calculation using the solid FEM model,  $L_{bc2}$  – calculation according to the methodology of this article

However, numerical calculations demonstrate that these effects indeed influence the strength of reinforced concrete columns. The results of numerical modeling confirm that the load-bearing capacity of a compressed column at an inclined section under transverse impact is determined by the stress-strain state of the concrete. The proposed model partially accounts for the effect of the closed transverse reinforcement contour through the parameter of the load intensity it resists. Nevertheless, the process of microcrack formation and the associated concrete dilation are not considered. The developed approach can serve as an additional tool in analyzing the robustness of buildings and structures subjected to emergency mechanical impacts of anthropogenic origin. Further development of the method is associated with its refinement for pylons and highly slender reinforced concrete columns. Another promising direction is the consideration of various types of initial and acquired damages, as well as the influence of existing strengthening systems on the load-bearing capacity of columns.

## CONCLUSION

1. A method for the analytical calculation of compressed-bent reinforced concrete elements under transverse impact has been developed, considering the bending and shear failure mechanisms.
2. The determination of load-bearing capacity accounts for the confinement of transverse concrete deformations under compression. This considers the spacing, diameter, and class of the transverse reinforcement. Limitations for the method's application have been defined – the design compressive force must be less than 80% of its ultimate value.
3. The proposed approach enables a significantly faster assessment of the mechanical safety level of reinforced concrete columns under horizontal dynamic loads compared to solid finite element modeling. The

developed relationships can be applied in designing preventive measures aimed at enhancing the resilience of buildings and structures to progressive collapse.

## REFERENCES

1. **Sun, J.-M., Yi, W.-J., Chen, H., Peng, F., Zhou, Y., Zhang, W.-X.** Dynamic Responses of RC Columns under Axial Load and Lateral Impact. *Journal of Structural Engineering*. 2023. 149(1). DOI:10.1061/jsendh/steng-11612.
2. **Li, X., Yin, Y., Li, T., Zhu, X., Wang, R.** Analytical Study on Reinforced Concrete Columns and Composite Columns under Lateral Impact. *Coatings*. 2023. 13(1). DOI:10.3390/coatings13010152.
3. **Zhao, W., Qian, J.** Resistance mechanism and reliability analysis of reinforced concrete columns subjected to lateral impact. *International Journal of Impact Engineering*. 2020. 136. DOI:10.1016/j.ijimpeng.2019.103413.
4. **Kashani, M.M., Crewe, A.J., Alexander, N.A.** Structural capacity assessment of corroded RC bridge piers. *Proceedings of the Institution of Civil Engineers: Bridge Engineering*. 2017. 170(1). DOI:10.1680/jbren.15.00023.
5. **Liu, B., Fan, W., Huang, X., Shao, X., Kang, L.** A Simplified Method to Predict Damage of Axially-Loaded Circular RC Columns Under Lateral Impact Loading. *International Journal of Concrete Structures and Materials*. 2020. 14(1). DOI:10.1186/s40069-020-00406-z.
6. **Gholipour, G., Zhang, C., Mousavi, A.A.** Effects of axial load on nonlinear response of RC columns subjected to lateral impact load: Ship-pier collision. *Engineering Failure Analysis*. 2018. 91. DOI:10.1016/j.engfailanal.2018.04.055.
7. **Zhao, W., Ye, J.** Dynamic behavior and damage assessment of RC columns subjected to lateral soft impact. *Engineering*

- Structures. 2022. 251. DOI:10.1016/j.engstruct.2021.113476.
8. **Alekseytsev A.V., Yurusov K.V.** A study on the bearing capacity of compressed corrosion-affected reinforced concrete elements subjected to transverse impulse loading. *Vestnik MGSU*. 2025;20(5):667-682. (In Russ.) <https://doi.org/10.22227/1997-0935.2025.5.667-682>
  9. **Mahmoud, K.A.** Lateral deformation behavior of eccentrically loaded slender RC columns with different levels of rotational end restraint at elevated temperatures. *Journal of Structural Fire Engineering*. 2021. 12(1). DOI:10.1108/JSFE-04-2020-0014.
  10. **Yilmaz, T., Kiraç, N., Anil, Ö.** Experimental investigation of axially loaded reinforced concrete square column subjected to lateral low-velocity impact loading. *Structural Concrete*. 2019. 20(4). DOI:10.1002/suco.201800276.
  11. **Fan, W., Liu, B., Consolazio, G.R.** Residual Capacity of Axially Loaded Circular RC Columns after Lateral Low-Velocity Impact. *Journal of Structural Engineering*. 2019. 145(6). DOI:10.1061/(asce)st.1943-541x.0002324.
  12. **Wang, X., Zhang, Y., Su, Y., Feng, Y.** Experimental Investigation on the Effect of Reinforcement Ratio to Capacity of RC Column to Resist Lateral Impact Loading. *Systems Engineering Procedia*. 2011. 1. DOI:10.1016/j.sepro.2011.08.007.
  13. **Anil, O., Cem Yilmaz, M., Barmaki, W.** Experimental and numerical study of RC columns under lateral low-velocity impact load. *Proceedings of the Institution of Civil Engineers: Structures and Buildings*. 2020. 173(8). DOI:10.1680/jstbu.18.00041.
  14. **Anil, Ö., Tuğrul Erdem, R., Tokgöz, M.N.** Investigation of lateral impact behavior of RC columns. *Computers and Concrete*. 2018. 22(1). DOI:10.12989/cac.2018.22.1.123
  15. **Demartino, C., Wu, J.G., Xiao, Y.** Response of shear-deficient reinforced circular RC columns under lateral impact loading. *International Journal of Impact Engineering*. 2017. 109. DOI:10.1016/j.ijimpeng.2017.06.011.
  16. **Zhou, X., Zhou, M., Luo, D., Wu, B., Liu, L.** Study on the nonlinear response and shear behavior of RC columns under lateral impact. *Structures*. 2021. 34. DOI:10.1016/j.istruc.2021.09.094.
  17. **Lai, D., Demartino, C., Xu, J., Xu, J., Xiao, Y.** GFRP bar RC columns under lateral low-velocity impact: an experimental investigation. *International Journal of Impact Engineering*. 2022. 170. DOI:10.1016/j.ijimpeng.2022.104365.
  18. **Swesi, A.O., Cotosovs, D.M., Val, D. V.** Effect of CFRP strengthening on response of RC columns to lateral static and impact loads. *Composite Structures*. 2022. 287. DOI:10.1016/j.compstruct.2022.115356.
  19. **Alekseytsev, A.V., Kvocak, K.V., Popov, D.S., Al Ali, M.** Dynamic behavior of a reinforced concrete slab of a pedestrian bridge with stiff rebars. *Magazine of Civil Engineering*. 2025. 18(1). Article no. 13303. DOI: 10.34910/MCE.133.3
  20. **Sidorov V.N., Badina E.S., Klimushkin D.O.** Modification of Rayleigh dissipation function for numerical simulation of internal damping in rod structures. *Vestnik MGSU*. 2024;19(6):960-970. (In Russ.) <https://doi.org/10.22227/1997-0935.2024.6.960-970>
  21. **Sidorov, V., Badina, E., & Tsarev, R.** Nonlocal in time dynamic deformation model and its calibration based on the beam vibration experiment results. *International Journal for Computational Civil and Structural Engineering*. 2025. 21(2):161-170. <https://doi.org/10.22337/2587-9618-2025-21-2-161-170>

## СПИСОК ЛИТЕРАТУРЫ

1. **Sun, J.-M., Yi, W.-J., Chen, H., Peng, F., Zhou, Y., Zhang, W.-X.** Dynamic Responses of RC Columns under Axial Load and Lateral Impact. *Journal of Structural Engineering*. 2023. 149(1). DOI:10.1061/jsendh/steng-11612.
2. **Li, X., Yin, Y., Li, T., Zhu, X., Wang, R.** Analytical Study on Reinforced Concrete Columns and Composite Columns under Lateral Impact. *Coatings*. 2023. 13(1). DOI:10.3390/coatings13010152.
3. **Zhao, W., Qian, J.** Resistance mechanism and reliability analysis of reinforced concrete columns subjected to lateral impact. *International Journal of Impact Engineering*. 2020. 136. DOI:10.1016/j.ijimpeng.2019.103413.
4. **Kashani, M.M., Crewe, A.J., Alexander, N.A.** Structural capacity assessment of corroded RC bridge piers. *Proceedings of the Institution of Civil Engineers: Bridge Engineering*. 2017. 170(1). DOI:10.1680/jbren.15.00023.
5. **Liu, B., Fan, W., Huang, X., Shao, X., Kang, L.** A Simplified Method to Predict Damage of Axially-Loaded Circular RC Columns Under Lateral Impact Loading. *International Journal of Concrete Structures and Materials*. 2020. 14(1). DOI:10.1186/s40069-020-00406-z.
6. **Gholipour, G., Zhang, C., Mousavi, A.A.** Effects of axial load on nonlinear response of RC columns subjected to lateral impact load: Ship-pier collision. *Engineering Failure Analysis*. 2018. 91. DOI:10.1016/j.engfailanal.2018.04.055.
7. **Zhao, W., Ye, J.** Dynamic behavior and damage assessment of RC columns subjected to lateral soft impact. *Engineering Structures*. 2022. 251. DOI:10.1016/j.engstruct.2021.113476.
8. **Alekseytsev A.V., Yurusov K.V.** A study on the bearing capacity of compressed corrosion-affected reinforced concrete elements subjected to transverse impulse loading. *Vestnik MGSU*. 2025;20(5):667-682. (In Russ.) <https://doi.org/10.22227/1997-0935.2025.5.667-682>
9. **Mahmoud, K.A.** Lateral deformation behavior of eccentrically loaded slender RC columns with different levels of rotational end restraint at elevated temperatures. *Journal of Structural Fire Engineering*. 2021. 12(1). DOI:10.1108/JSFE-04-2020-0014.
10. **Yilmaz, T., Kiraç, N., Anil, Ö.** Experimental investigation of axially loaded reinforced concrete square column subjected to lateral low-velocity impact loading. *Structural Concrete*. 2019. 20(4). DOI:10.1002/suco.201800276.
11. **Fan, W., Liu, B., Consolazio, G.R.** Residual Capacity of Axially Loaded Circular RC Columns after Lateral Low-Velocity Impact. *Journal of Structural Engineering*. 2019. 145(6). DOI:10.1061/(asce)st.1943-541x.0002324.
12. **Wang, X., Zhang, Y., Su, Y., Feng, Y.** Experimental Investigation on the Effect of Reinforcement Ratio to Capacity of RC Column to Resist Lateral Impact Loading. *Systems Engineering Procedia*. 2011. 1. DOI:10.1016/j.sepro.2011.08.007.
13. **Anil, O., Cem Yilmaz, M., Barmaki, W.** Experimental and numerical study of RC columns under lateral low-velocity impact load. *Proceedings of the Institution of Civil Engineers: Structures and Buildings*. 2020. 173(8). DOI:10.1680/jstbu.18.00041.
14. **Anil, Ö., Tuğrul Erdem, R., Tokgöz, M.N.** Investigation of lateral impact behavior of RC columns. *Computers and Concrete*. 2018. 22(1). DOI:10.12989/cac.2018.22.1.123
15. **Demartino, C., Wu, J.G., Xiao, Y.** Response of shear-deficient reinforced circular RC columns under lateral impact loading. *International Journal of Impact Engineering*. 2017. 109. DOI:10.1016/j.ijimpeng.2017.06.011.

16. **Zhou, X., Zhou, M., Luo, D., Wu, B., Liu, L.** Study on the nonlinear response and shear behavior of RC columns under lateral impact. *Structures*. 2021. 34. DOI:10.1016/j.istruc.2021.09.094.
17. **Lai, D., Demartino, C., Xu, J., Xu, J., Xiao, Y.** GFRP bar RC columns under lateral low-velocity impact: an experimental investigation. *International Journal of Impact Engineering*. 2022. 170. DOI:10.1016/j.ijimpeng.2022.104365.
18. **Swesi, A.O., Cotsovos, D.M., Val, D. V.** Effect of CFRP strengthening on response of RC columns to lateral static and impact loads. *Composite Structures*. 2022. 287. DOI:10.1016/j.compstruct.2022.115356.
19. **Alekseytsev, A.V., Kvocak, K.V., Popov, D.S., Al Ali, M.** Dynamic behavior of a reinforced concrete slab of a pedestrian bridge with stiff rebars. *Magazine of Civil Engineering*. 2025. 18(1). Article no. 13303. DOI: 10.34910/MCE.133.3
20. **Sidorov V.N., Badina E.S., Klimushkin D.O.** Modification of Rayleigh dissipation function for numerical simulation of internal damping in rod structures. *Vestnik MGSU*. 2024;19(6):960-970. (In Russ.) <https://doi.org/10.22227/1997-0935.2024.6.960-970>
21. **Sidorov, V., Badina, E., & Tsarev, R.** Nonlocal in time dynamic deformation model and its calibration based on the beam vibration experiment results. *International Journal for Computational Civil and Structural Engineering*. 2025. 21(2):161-170. <https://doi.org/10.22337/2587-9618-2025-21-2-161-170>

---

*Alekseytsev Anatoly Viktorovich*, doctor of technical sciences, associated professor, professor of the department "Reinforced concrete and stone structures"; National Research Moscow State Technical University (NRU MGSU), Russia, Moscow, Yaroslavskoe sh., 26, Scopus ID: 57191530761, Researcher ID: I-3663-2017, ORCID: 0000-0002-4765-5819, e-mail: [alekseytsevav@mail.ru](mailto:alekseytsevav@mail.ru).

*Алексейцев Анатолий Викторович*, доктор технических наук, доцент, профессор кафедры «Железобетонные и каменные конструкции»; Национальный исследовательский московский государственный технический университет (НИУ МГСУ), Россия, г. Москва, Ярославское ш., 26, Scopus ID: 57191530761, Researcher ID: I-3663-2017, ORCID: 0000-0002-4765-5819, e-mail: [alekseytsevav@mgsu.ru](mailto:alekseytsevav@mgsu.ru).

*Valentina M. Tushina*, docent, candidate of technical sciences, associated professor of department "Architectural and construction design and physics of the environment"; National Research Moscow State University of Civil Engineering (National Research University); Russia, 129337 Moscow, Yaroslavskoe sh., 26. Scopus ID: 56296961500; Researcher ID: AAD-8968-2022; ORCID: 0000-0003-0328-0848. e-mail: [valmalaz@mail.ru](mailto:valmalaz@mail.ru)

*Туснина Валентина Матвеевна*, доцент, кандидат технических наук, доцент кафедры «Архитектурно-строительное проектирование и физика среды»; Национальный исследовательский московский государственный строительный университет (НИУ МГСУ); Россия, 129337 Москва, Ярославское шоссе, 26; Scopus ID: 56296961500; Researcher ID: AAD-8968-2022; ORCID: 0000-0003-0328-0848. e-mail: [valmalaz@mail.ru](mailto:valmalaz@mail.ru)